Control Strategy and Design for a Packed-Bed Thermochemical Heat Storage Reactor

Michael Wild[1]

[1] Department of Mechanical and Process Engineering, ETH Zürich, 8092 Zurich, Switzerland

Abstract

The concept of a controllable combined sensible-thermochemical thermal energy storage for utilization with concentrated solar power plants is presented. An encapsulated thermochemical storage utilizing reversible gas-solid reactions is coupled to a packed-bed sensible storage using rocks as storage media. The thermal decomposition of manganese oxide is chosen as a demonstration reaction. A simplified heat transfer model of the thermochemical section is implemented in Simulink. The equations that govern this model are presented. This implementation allows for rapid iterations to find a controller design that stabilizes the storage outflow temperature shows robust and exact performance over a wide range of operating parameters. The controller consists of feedforward and feedback portions with integrator windup protection. This controller design is subsequently ported to an existing simulation framework that resolves the domain to a higher degree of accuracy and implements temperature-dependent material properties. The resulting controller-TCS combination is limited primarily by finite reaction rates and heat transfer to the surrounding heat transfer fluid. For all practical applications, the thermochemical section is able to stabilize (or actively control) the combined storage outflow temperature.

Keywords: Solar, Thermal Energy Storage, Thermochemical Storage, Controller Design

Nomenclature

Acronyms		*Variables*	
CSP	Concentrated Solar Power	T	Temperature [K]
TES	Thermal Energy Storage	t	Time [s]
HTF	Heat Transfer Fluid	M	Molar Weight [g ·mol]
SHS	Sensible Heat Storage	c_p	Specific Heat Capacity [J·mol^{-1}·K^{-1}]
TCS	Thermochemical Heat Storage	V	Volume [m^3]
Subscripts		ρ	Density [kg·m^{-3}]
r	Reactor	$\dot{Q}$	Rate of Heat Flow [W]
f	Fluid	X	Reaction Extent [-]
fb	Feedback	k_0	Rate Constant [s^{-1}]
ff	Feedforward	E_a	Activation Energy [J·mol^{-1}]
i	Cell Index	R	Universal Gas Constant [J·mol^{-1}·K^{-1}]
set	Setpoint	a,b,s, γ_1	Empirically Fitted Parameters [-]
ht	Heat Transfer	γ_2	Empirically Fitted Parameter [K]
diff	Difference	p	Pressure [Pa]
in	Inlet	ΔH_R	Reaction Enthalpy [J·mol^{-1}]
out	Outlet	k_h	Interphase Heat Transfer Coefficient [W·K^{-1}]
chem	Chemical	τ	PID Integrator Boundary [K·s]

1. Introduction

Concentrated solar power (CSP) plants use mirror optics to concentrate solar radiation into a receiver or reactor. The resulting high temperature heat can be used to generate electricity or drive energy-intensive processes in a carbon-neutral way. Although industrially deployed, CSP plants are limited by the intermittency constraints of solar radiation – clouds, day/night cycles and seasonal variations lead to low utilization factors and unplannable generation. Effective use of CSP technology thus requires the ability to store solar heat and release it once it's needed. Thermal energy storage (TES) directly stores solar heat and therefore avoids inefficient transformations into other forms of energy. Three forms of TES are generally considered: sensible, latent and thermochemical (Kuravi et al., 2013). Sensible heat storage (SHS) utilizes the heat capacity of the storage material, while latent heat utilizes the energy needed to drive a phase change in the storage material. Thermochemical storage (TCS) stores heat in the reaction enthalpy of reversible endothermic/exothermic reactions. In the case of gas-solid dissociation reactions such as the calcination/carbonation of limestone, the reaction equilibrium and thus indirectly the reaction rate can be

doi:10.18086/swc.2019.21.06 Available at http://proceedings.ises.org

influenced by adjusting the gas pressure inside the storage reactor.

Thermochemical storage on its own is difficult since most reactions have a comparatively narrow operating temperature range. There are two general to solutions to this problem. In theory, a stack of different TCS materials operating in complementing temperature ranges could store heat over the whole temperature range (Agrafiotis et al., 2016), however it is exceedingly difficult to find materials that react at low temperatures and demonstrate high cycle stability. Alternatively, the TCS can be coupled to a packed-bed SHS. In such a configuration, the TCS section acts as a control unit to the SHS and could alleviate the drawbacks of such a storage, i.e. thermocline degradation and associated heat transfer fluid (HTF) outlet temperature drop.

The envisioned TCS reactor section consists of layered arrays of reactor tubes that are in a crossflow configuration to the HTF flowing through the combined TCS/SHS system. Fig. 1 shows a schematic view of the TCS section that is added on top of the SHS. The reactor tubes consist of a gas-tight outer shell, the powdered/granulated solid reactants and a concentric, porous gas-feeding tube. During charging, heat is conducted inwards, dissociating the solid reactant. The produced gas is drawn out through the center tube. In the discharging phase, the gas is pumped back into the reactor under slightly higher pressure, where it recombines with the solid.

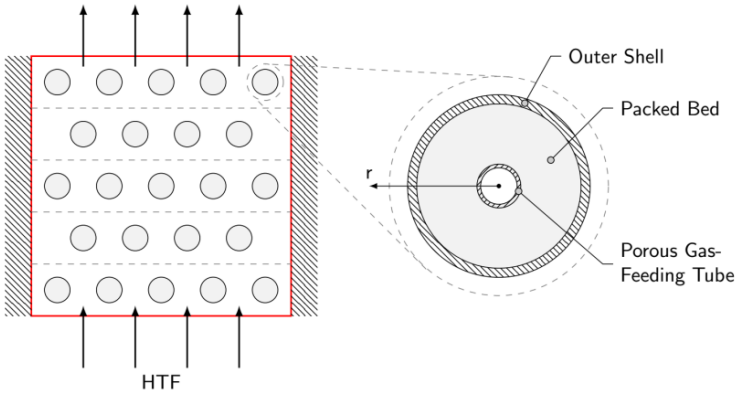

Fig. 1: Schematic configuration of the combined sensible-thermochemical thermal energy storage system. The thermochemical storage (TCS) stack is located on top of the sensible heat storage (SHS). The TCS itself consists of stacked layers of tubes. A single tube consists of a gas-tight shell containing the powdered bed of solid reactants and an inner concentric porous gas-feeding tube.

In order to achieve the desired HTF output temperature, the reactor pressure has to be actively controlled. To find a suitable control strategy, first a rapid iteration testbed simulation was constructed based on a very simplified model of TCS reactor stack. Then, the controller that was designed in this fashion was implemented into an existing simulation environment that resolves heat and mass transfer with higher granularity.

2. Rapid Iteration Control Strategy Testbed

From a control standpoint, the only sensor input reasonably available is the temperature of the HTF outflow temperature after the TCS section. The output of the control unit has to be the reactor pressure(s). For the sake of a technically simple and efficient system, a single compressor is adjusting the pressure in all reactors simultaneously. Since the reaction rate in each reactor depends on multiple variables (e.g. reaction extent and local temperature), in general each layer of the TCS stack will react differently to a given pressure.

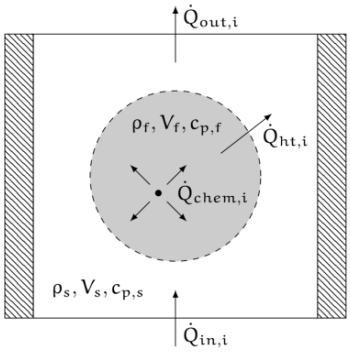

Fig. 2: Control volume consisting of a HTF cell surrounding a single reactor tube with no spatial resolution. Heat is emitted or consumed by the chemical reaction in the tube and convected to the HTF that flows vertically.

To rapidly iterate control system designs, a simplified model of a tubular reactor was constructed, based on prior work. The model recognizes two regions (tubular reactor and HTF envelope) and has no spatial resolution in the respective regions. Figure 2 shows the chosen control volume for a single tube. Please refer to the nomenclature for a detailed description of the terms.

$$\frac{\partial T_{\mathrm{r},i}}{\partial t} = \frac{M_{\mathrm{r}}}{c_{\mathrm{p,r}} V_{\mathrm{r}} \rho_{\mathrm{r}}} \left(\dot{Q}_{\mathrm{chem},i} - \dot{Q}_{\mathrm{ht},i} \right) \quad (1)$$

$$\frac{\partial T_{\mathrm{f},i}}{\partial t} = \frac{1}{c_{\mathrm{p,f}} V_{\mathrm{f}} \rho_{\mathrm{f}}} \left(\dot{Q}_{\mathrm{in},i} - \dot{Q}_{\mathrm{out},i} + \dot{Q}_{\mathrm{ht},i} \right) \quad (2)$$

$$\frac{\partial \mathrm{X}_i}{\partial t} = k_0 \exp\left(\frac{E_{\mathrm{a}}}{R T_{\mathrm{r},i}}\right) \mathrm{X}_i^a (1 - \mathrm{X}_i)^b \left| 1 - \frac{p_i}{p_{\mathrm{eq},i}} \right|^s \quad (3)$$

$$p_{\mathrm{eq},i} = \exp\left(\gamma_1 + \frac{\gamma_2}{T_{\mathrm{r},i}}\right) \quad (4)$$

$$\dot{Q}_{\mathrm{chem},i} = \frac{\rho_{\mathrm{r}} V_{\mathrm{r}}}{M_{\mathrm{r}}} \Delta H_{\mathrm{R}} \frac{\partial \mathrm{X}_i}{\partial t} \quad (5)$$

$$\dot{Q}_{\mathrm{ht},i} = k_h \cdot (T_{\mathrm{r},i} - T_{\mathrm{f},i}) \quad (6)$$

$$\dot{Q}_{\mathrm{out},i} = \dot{Q}_{\mathrm{in},i} + \dot{Q}_{\mathrm{ht},i} = \dot{Q}_{\mathrm{in},i+1} \quad (7)$$

Eqs. 1 and 2 represent the energy balance of the tube and the HTF, respectively. Eq. 3 describes the reaction rate which is dependent on reactor temperature, reaction extent and gas pressure. The equilibrium gas pressure for a given temperature is given in eq. 4. The integrated heat fluxes are described by eqs. 5-7. The direction of heat fluxes is indicated by the direction of the associated arrows in Figure 2.

This model was implemented in Simulink (MATLAB toolbox) using numerical values corresponding to the thermal decomposition of manganese(III) oxide:

$$6\mathrm{Mn_2O_3} \leftrightarrow \mathrm{O_2} + 4\mathrm{Mn_3O_4} \quad (8)$$

Following this implementation, ten such encapsulated reactor models were linked together via eq. 7 to form a TCS stack. Subsequently, the heat flux into the first layer is defined as the outlet of the SHS section, while the outflow of the last layer defines the combined-system output that is used as the control system input.

3. Controller Design

The control of such a system is not straightforward, since it is highly nonlinear. The final controller consists of three main parts: (1) a standard PID controller, (2) a feed-forward portion and (3) an integrator windup protection. Figure 3 shows the control system block diagram that was implemented. The reactor pressure is directly controlled using an addition of feedforward (FF) and feedback (PID) controller pressures. The feedforward pressure is directly related to the equilibrium pressure of the reaction at the setpoint temperature (analogous to eq. 4), i.e.

$$P_{\mathrm{ff}} = \exp\left(\gamma_1 + \frac{\gamma_2}{T_{\mathrm{set}}}\right) \quad (9)$$

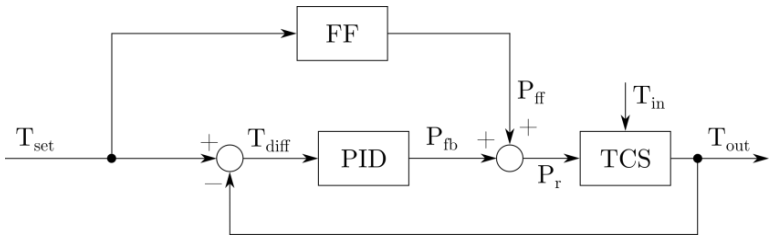

Fig. 3: Control system block diagram containing the implemented controller. The setpoint temperature (T_{set}) is fed into the feedforward controller (FF) which produces the feedforward pressure (P_{ff}). The temperature difference (T_{diff}) between TCS outlet temperature (T_{out}) and setpoint temperature is the input to the PID controller which produces the feedback pressure (P_{fb}). Feedforward and feedback pressure are added to yield the reactor pressure (P_r). The TCS inlet temperature (T_{in}) is conceptually modelled as a disturbance to the system since it is not known *a priori*.

The PID controller is described by eq. 10:

$$P_{\mathrm{fb}} = T_{\mathrm{diff}} \cdot \mathrm{P} + \max\left(\tau, \int_0^t T_{\mathrm{diff}}\, dt\right) \cdot \mathrm{I} + \frac{\partial T_{\mathrm{diff}}}{dt} \cdot \mathrm{D} \quad (10)$$

where P,I and D are the respective numerical values for the proportional, integral and differential portions of the controller. The numerical value of τ bounds the rate at which the integrator can fill.

The rationale for this feedforward/feedback combination is that in the case of an infinitely fast reaction and no heat transfer resistance between reactor and HTF, the feedforward pressure (eq. 9) alone will perfectly stabilize the HTF outlet temperature. In a more realistic case, the feedback loop accounts for the (conceptual) disturbance of the TCS inlet temperature, the finite (and state-dependent) reaction rates and heat transfer limitations. All of these effects lead to a necessarily higher reactor pressure than the equilibrium pressure, therefore the feedforward provides the base pressure while the feedback loop handles the fluctuations.

Figure 4 shows the results of a representative simulation where the SHS section delivers a constant TCS inlet temperature of 1035 K which in turn has to be raised to a constant TCS outlet temperature of 1050 K. Since the reaction rate in the vicinity of equilibrium conditions approximately scales with the temperature difference to the equilibrium temperature, the first (bottom) reactor outputs the most heat during the beginning of the discharging phase, while the last (top) reactor only contributes very little. One by one, reactors are depleted and the load shifts upwards. At the end of the discharge, a physical limit to the reactor pressure is reached and the outlet temperature starts to sink rapidly.

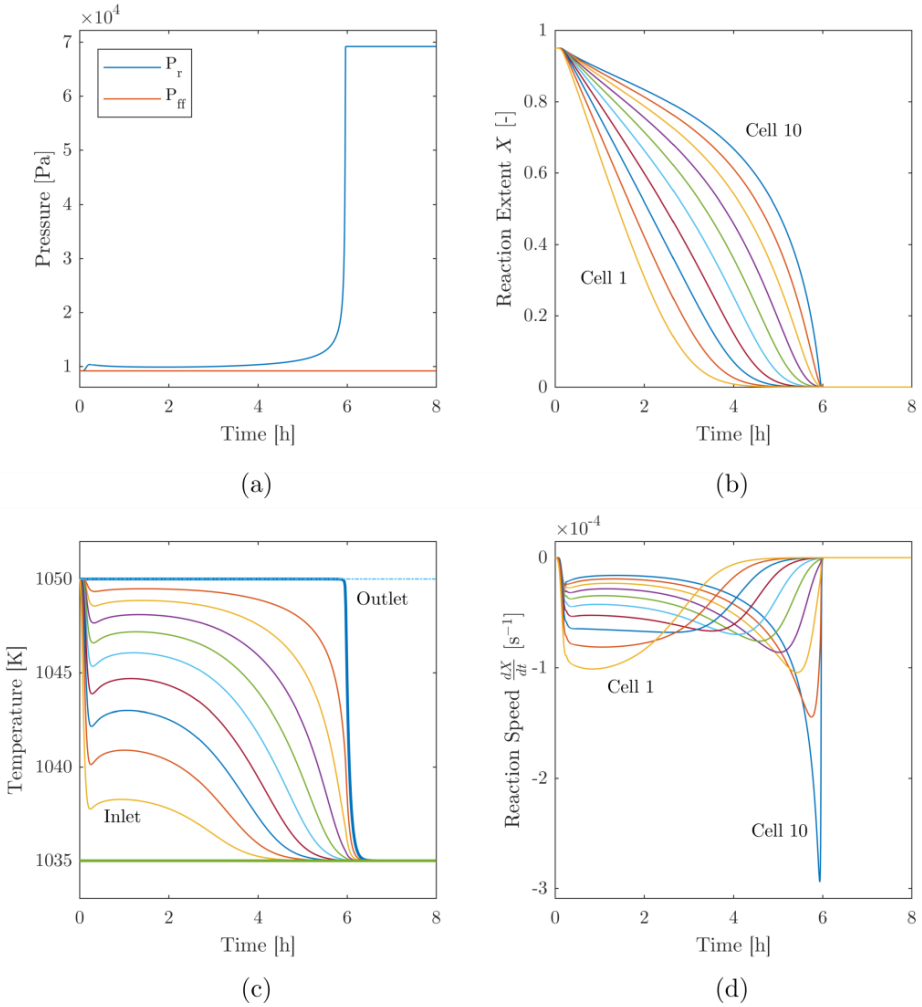

Fig. 4: Representative run of a 10-cell Simulink TCS model during the discharging phase with numerical values for the decomposition of manganese oxide. The SHS outlet temperature (equivalent to TCS inlet temperature) is set to 1035 K while the setpoint temperature for the TCS outlet is set at constant 1050 K. The plots show: (a) the evolution of the uniform reactor pressure with the contribution of the constant feedforward portion indicated, (b) the reaction extent of the cells over time, (c) the fluid temperature of the cells over time, (d) the reaction speed of the cells over time. After approximately 6 hours the last storage cell is depleted.

4. Controller Verification

To verify its functionality, the controller design that was found in the last section was implemented into an existing FORTRAN simulation framework based on prior work (Ströhle et al., 2017, 2013). The underlying model still does

not resolve any spatial gradients inside the tubular reactors but accounts for the fluid flow around the reactors in a more complex way (based on Žukauskas, 1973) and allows for higher numerical accuracy. It also implements temperature-dependent material properties and reaction enthalpy. The input to the controller was delayed by multiple seconds to simulate a more realistic behavior.

The PID controller parameters themselves are obviously dependent on the system dimensions and requirements; still it was found that a wide range of parameters was able to control the system to a satisfying degree. This is attributed to the fact that the timescale of the system (order or hours) is vastly longer than the timescale of the controller (order of milliseconds).

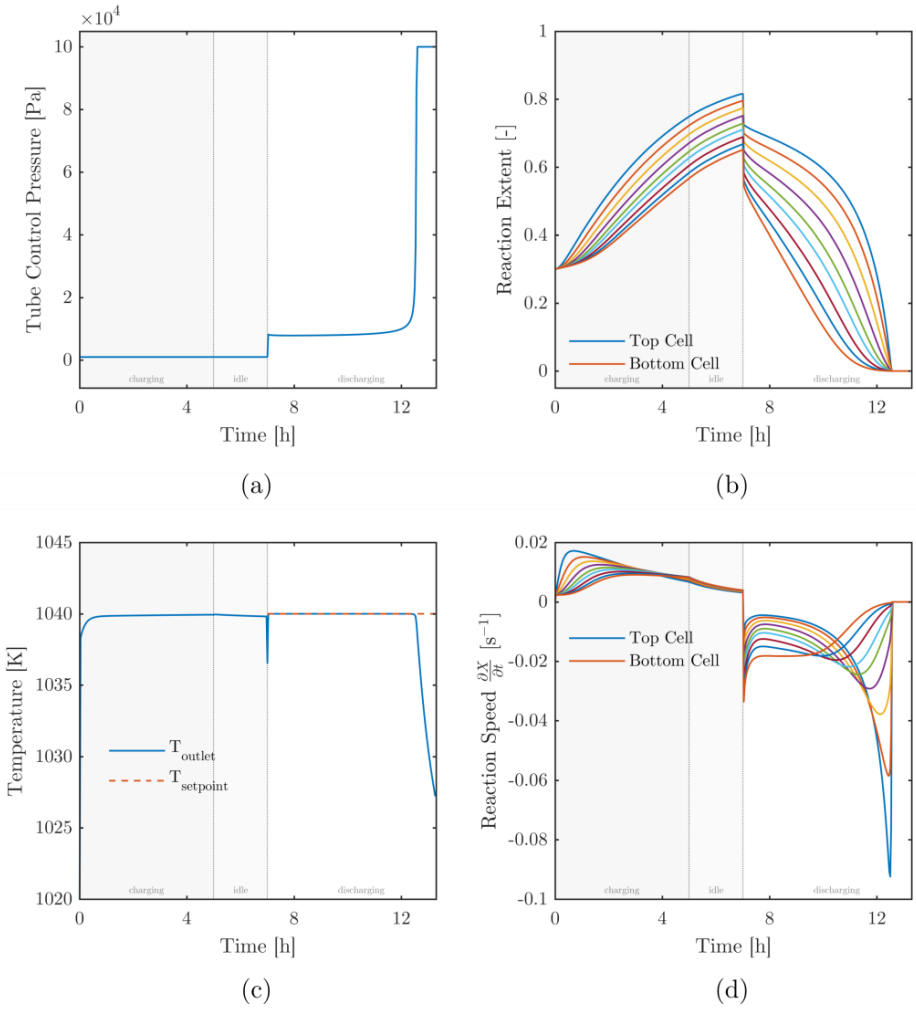

Fig. 5: Representative run of a simulation using the complete model including a charging, idle and discharging phase. During the charging phase, the pressure in the reactors is set to a reasonable partial vacuum pressure to encourage faster charging. The plots show: (a) the evolution of the uniform reactor pressure, (b) the reaction extent of selected cells over time, (c) the fluid temperature of the outlet over time, (d) the reaction speed of selected cells over time. Note the similarity to the results shown in Figure 3.

A variety of input parameters (e.g. HTF massflow, setpoint temperature) as well as disturbances (TCS inlet temperature variations) were tested. Additionally, various physical properties were altered in a reasonable range, e.g. a change in the reaction enthalpy or reaction rate, in order to simulate uncertainties and measurement errors in the characterization of the used materials. The control system was able to compensate for all of these cases with relative ease. Depending on the projected use case (e.g. constant or variable outlet temperature), the parameters can be fine-tuned to yield a better result.

5. Summary and Future Work

A system for the active control of the HTF outflow temperature of a combined sensible/thermochemical heat storage has been developed. Using a simplified model, various options were explored and refined. A viable option was found consisting of a feedback/feedforward combination with integrator windup protection. This was then implemented in an existing simulation that resolves heat and mass transfer on a more fundamental level and provides an increased

amount of granularity. The used controller showed very robust performance and high accuracy as it was able to handle a wide variety of input conditions and disturbances to the system.

As a further step, a model resolving the heat and mass transfer within the reactor tube is under development. Depending on limitations inside the reactor, delay times with respect to the controller and boundaries to the operating envelope are anticipated. However, appropriate tuning of the controller parameters is expected to resolve this.

6. Acknowledgements

The financial support of this project by the Swiss National Science Foundation (Grant Nr. 173438) is gratefully acknowledged.

I thank Prof. Aldo Steinfeld for his comments that have greatly improved this manuscript.

I thank Dr. Zoran Jovanovic and Dr. Andreas Haselbacher for sharing their great knowledge on the topic of thermal storage.

I thank Dr. Stefan Ströhle for his explanations and help in working with the FORTRAN simulation described in section 5.

7. References

Agrafiotis, C., Roeb, M., Sattler, C., 2016. Exploitation of thermochemical cycles based on solid oxide redox systems for thermochemical storage of solar heat. Part 4: Screening of oxides for use in cascaded thermochemical storage concepts. Sol. Energy 139, 695–710. https://doi.org/10.1016/j.solener.2016.04.034

Kuravi, S., Trahan, J., Goswami, D.Y., Rahman, M.M., Stefanakos, E.K., 2013. Thermal energy storage technologies and systems for concentrating solar power plants. Prog. Energy Combust. Sci. 39, 285–319. https://doi.org/10.1016/j.pecs.2013.02.001

Ströhle, S., Haselbacher, A., Jovanovic, Z.R., Steinfeld, A., 2017. Upgrading sensible-heat storage with a thermochemical storage section operated at variable pressure: An effective way toward active control of the heat-transfer fluid outflow temperature. Appl. Energy 196, 51–61. https://doi.org/10.1016/j.apenergy.2017.03.125

Ströhle, S., Jovanovic, Z., Haselbacher, A., Steinfeld, A., 2013. One-Dimensional Heat and Mass Transfer and Discrete Granule Model of a Tubular Packed-Bed Reactor for Thermochemical Storage of Solar Energy, in: Volume 1: Heat Transfer in Energy Systems; Thermophysical Properties; Theory and Fundamental Research in Heat Transfer. ASME, pp. 1–10. https://doi.org/10.1115/HT2013-17301

Žukauskas, A., 1973. Heat transfer from tubes in crossflow. Adv. Heat Transf. 8, 93–160. https://doi.org/10.1016/S0065-2717(08)70038-8